benzhydrol **25** as a yellow-brown powder (0.215 g, 14%), mp 151-154 °C. IR: 3600-3150 (m, O-H str), 1533 (s, asymm N-O str), 1352 cm^{-1} (m, symm N-O str). ^1H NMR: δ (Me_2CO), 6.37 (1 H, d (J = 6 Hz), OH (D_2O exch)), 7.35 (1 H, d (J = 6 Hz), C*H*OH), 7.91 (2 H, t (J_o = 8 Hz), 2 × H para to -CHOH), 8.13 (4 H, d (J_o = 8 Hz), 2 × 2 H ortho to NO_2). ^{13}C NMR: δ (Me_2CO), 64.95 (CHOH), 128.22 (C para to CHOCOR), 128.70 (C meta to CHOH), 131.66 (C ipso to CHOCOR), 151.05 (C ipso to NO_2). UV: ϵ_{254} 12021.

Preparation of *N*-[[(2,6-Dinitrophenyl)-1-(2',6'-dinitrophenyl)methoxy]carbonyl]cyclohexylamine (23). To a solution of 2,6-dinitro-α-(2',6'-dinitrophenyl)benzenemethanol (**25**) (0.130 g, 0.354 mmol) in anhydrous tetrahydrofuran (25 mL) at room temperature under nitrogen was added an ethereal solution of methyllithium (1.50 M, 24 μL, 0.035 mmol). The resulting solution was stirred under these conditions for 2 h and then treated dropwise with a solution of cyclohexyl isocyanate (45 μL, 0.044 g, 0.354 mmol) in dry tetrahydrofuran (10 mL). Once the addition was complete, the solution was heated at reflux for 12 h, cooled to room temperature, and concentrated in vacuo. The residue was taken up in chloroform (50 mL) and washed with water (2 × 15 mL) and brine (1 × 10 mL). After drying ($MgSO_4$), removal of the solvent in vacuo gave a brown oil (0.210 g), which on flash chromatography (75% CH_2Cl_2/25% hexane) followed by recrystallization (ether) afforded the desired carbamate **23** as an almost white solid (0.090 g, 52%), mp 180-182 °C. Anal. Calcd for $C_{20}H_{19}N_5O_{10}$ (489.39): C, 49.08; H, 3.91; N, 14.31. Found: C, 49.29; H, 4.03; N, 14.15. IR: 3409 (m, N-H str), 1730 (m, C=O str), 1540 (s, asymm N-O str), 1360 cm^{-1} (m, symm N-O str). ^1H NMR: δ 1.02-1.32 (5 H, m, 5 cyclohexyl H), 1.55-1.70 (3 H, m, 3 cyclohexyl H), 1.81-1.92 (2 H, m, 2 cyclohexyl H), 3.05-3.15 and 3.24-3.35 (total 1 H, each br m, cyclohexyl ring methine), 5.25-5.35 and 5.45-5.56 (total 1 H, each br m, -NH-), 7.72 (2 H, t (J_o = 8 Hz), 2 × H para to -CHOCONHR), 7.97 (4 H, d (J_o = 8 Hz), 2 × 2 H ortho to NO_2), 8.02 (1 H, s, -C*H*OCONHR). ^{13}C NMR: δ 24.47 (cyclohexyl C β to substituent), 25.20 (cyclohexyl C γ to substituent), 32.68 (cyclohexyl C α to substituent), 50.34 (substituted cyclohexyl C), 66.48 (*C*HOCOR), 125.43 (C para to CHOCOR), 127.96 (C meta to CHOCOR), 130.70 (C ipso to CHOCOR), 150.40 (C ipso to NO_2), 152.73 (CHO*C*OR). UV: ϵ_{254} 12974.

Acknowledgment. Financial support of this research by the Office of Naval Research (Grant N00014-91-J-1338) and through a gift from IBM Corp. (Materials and Processing Sciences Program) is gratefully acknowledged.

Functional Group Substitutions as Probes of Hydrogen Bonding between GA Mismatches in RNA Internal Loops

John SantaLucia, Jr.,[†] Ryszard Kierzek,[‡] and Douglas H. Turner*,[†]

Contribution from the Department of Chemistry, University of Rochester, Rochester, New York 14627, and Institute of Bioorganic Chemistry, Polish Academy of Sciences, 60-704 Poznan, Noskowskiego 12/14, Poland. *Received August 29, 1990*

Abstract: The contribution of hydrogen bonding to the stability of GA mismatches in RNA is investigated by making functional group substitutions. Such substitutions are made possible by the chemical synthesis of RNA; chemical incorporation of purine riboside and 2-aminopurine riboside into oligoribonucleotides is reported. In particular, replacing the 6-amino groups of internal loop adenosines with hydrogen atoms in $(rGCGAGCG)_2$, $(rGGCGAGCC)_2$, $(rGCAGGCG)_2$, and $(rCGCAGGCG)_2$ destabilizes the duplexes by 2.8, 3.0, 3.2, and 2.7 kcal/mol, respectively. The results suggest hydrogen bonding within each GA mismatch contributes at least -1.4 kcal/mol to duplex stability. Results on control sequences in which the internal loop residues are changed to inosine, 2-aminopurine riboside, or purine riboside are consistent with this interpretation. The results provide insight into the source of the unusual stability of RNA duplexes with internal loops containing GA mismatches (SantaLucia, J., Jr.; Kierzek, R.; Turner, D. H. *Biochemistry* **1990**, *29*, 8813-8819). In contrast to GA mismatches in internal loops, hydrogen bonding between GA mismatches at the ends of oligonucleotide helices does not make a large contribution to helix stability. The implications of these results for predicting RNA structure are discussed.

Introduction

Hydrogen bonds play an important role in the folding and molecular recognition of biological macromolecules.[1] The quantitative contributions of hydrogen bonds to structural stability, however, have been disputed.[2,3] Studies on small molecules have been interpreted as indicating either a favorable[4,5] or a negligible[6] free energy contribution from hydrogen bonds. Site-specific mutations in proteins have been used to remove specific functional groups involved in hydrogen bonding.[7] The results suggest hydrogen bonds between noncharged amino acid residues contribute from -0.5 to -1.2 kcal/mol to substrate binding.[3] Removal of specific functional groups has also been used to probe for hydrogen bonding in nucleic acid base pairs.[8] The results suggest a hydrogen bond can contribute from -0.5 to -2.0 kcal/mol to the stability of a base pair.

Internal loops form in double helical RNA when a helix is interrupted by unpaired nucleotides on both strands and are common in natural RNA molecules.[9,10] Predictions of RNA structure from sequence are sensitive to parameters for internal loops,[11] but little is known about the interactions determining loop stability. Current models of internal loops do not include hydrogen bonding interactions within the loop.[11-13] We recently discovered,

* Author to whom correspondence should be addressed.
† University of Rochester.
‡ Polish Academy of Sciences.

(1) Cantor, C. R.; Schimmel, P. R. *Biophysical Chemistry Part I: The Conformation of Biological Macromolecules*; W. H. Freeman: San Francisco, 1980.
(2) Jencks, W. P. *Catalysis in Chemistry and Enzymology*; McGraw-Hill: New York, 1969.
(3) Fersht, A. R. *Trends Biochem. Sci.* **1987**, *12*, 301-304.
(4) Robinson, D. R.; Jencks, W. P. *J. Am. Chem. Soc.* **1965**, *87*, 2462-2470.
(5) Schellman, J. A. *C. R. Trav. Lab. Carlsberg. Ser. Chim.* **1955**, *29*, 223-229.
(6) Klotz, I. M.; Franzen, J. S. *J. Am. Chem. Soc.* **1962**, *84*, 3461-3466.
(7) Fersht, A. R.; Shi, J.-P.; Knill-Jones, J.; Lowe, D. M.; Wilkinson, A. J.; Blow, D. M.; Brick, P.; Wage, M. M. Y.; Winter, G. *Nature (London)* **1985**, *314*, 235-238.
(8) Turner, D. H.; Sugimoto, N.; Kierzek, R.; Dreiker, S. D. *J. Am. Chem. Soc.* **1987**, *109*, 3783-3785.
(9) Woese, C. R. *Microbiol. Rev.* **1983**, *51*, 221-271.
(10) Noller, H. F. *Annu. Rev. Biochem.* **1984**, *53*, 119-162.
(11) Turner, D. H.; Sugimoto, N.; Freier, S. M. *Annu. Rev. Biophys. Biophys. Chem.* **1988**, *17*, 167-192.

0002-7863/91/1513-4313$02.50/0

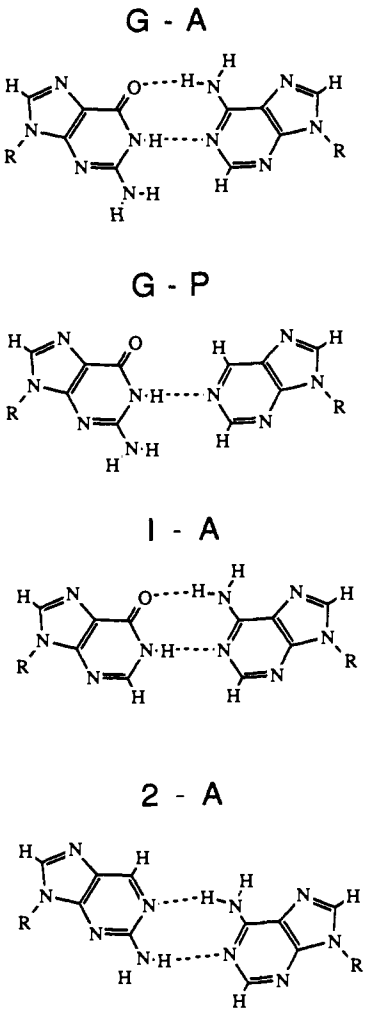

Figure 1. Functional group substitutions (top to bottom): GA mismatch in anti-anti conformation; GP mismatch, i.e. adenine 6-amino group removed; IA mismatch, i.e. guanine 2-amino group removed; 2A mismatch, i.e. guanine O6 and imino proton removed.

however, that internal loops containing 2 GA mismatches are more than 2 kcal/mol more stable than those containing 2 AA mismatches.[14] This suggests hydrogen bonding in GA mismatches may make a large contribution to internal loop stability.

In this paper, the thermodynamic effect of hydrogen bonding in GA mismatches is studied by replacing adenosine with purine riboside (an A→P substitution). This substitution replaces the 6-amino group of adenine with a hydrogen atom, thus eliminating hydrogen bonding at this position (see Figure 1). Other substitutions investigated include guanosine to inosine (G→I) and guanosine to 2-aminopurine riboside (G→2). Such substitutions are made possible by the chemical synthesis of RNA;[15,16] chemical incorporation of purine riboside and 2-aminopurine riboside into oligoribonucleotides is reported. The results indicate hydrogen bonds contribute approximately −1.4 kcal/mol to the stability of a GA mismatch in an internal loop but do not contribute significantly to the stability of a GA mismatch at the terminus of an oligomer duplex. Since GA mismatches are common in internal loops,[9,10] the results suggest inclusion of parameters for hydrogen bonding will improve predictions of RNA secondary structure.[11]

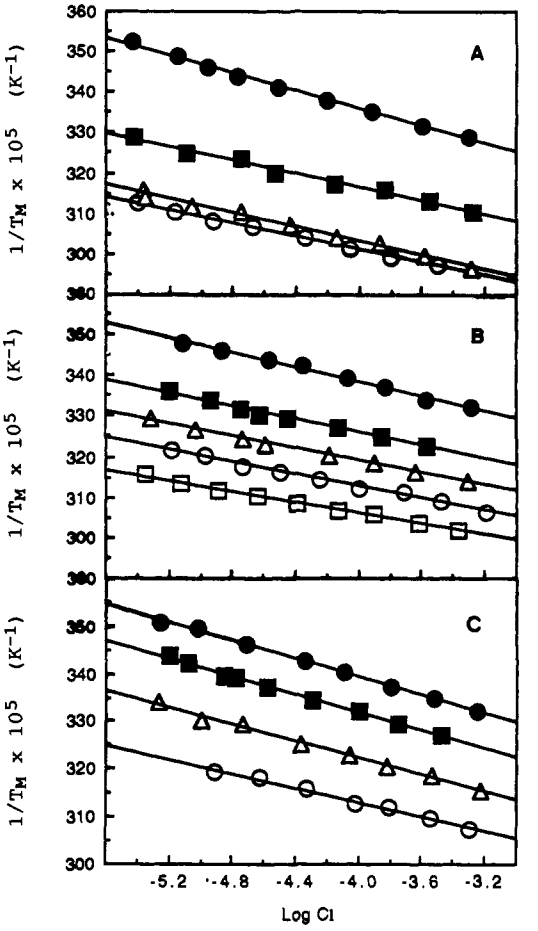

Figure 2. Reciprocal melting temperature vs log (concentration) plots for (A) rGCGAGCG (■), rGCGPGCG (●), rGAGCGCGA (○), and rGPGCGCGP (△); (B) rGCAGGCG (△), rGCPGGCG (●) (low-melting transition), rGCAIGCG (○), rCGCAIGCG (□), and rCGCPGGCG (■); and (C) rGC2AGCG (△), rGCIAGCG (○), rGCPPGCG (●), and rGCIPGCG (■).

Results

In our previous study, thermodynamic parameters were measured for the following duplexes.[14]

5′ GC^{GA}GCG 3′ 5′ GC^{AG}GCG 3′ 5′ GGC^{GA}GCC 3′ 5′ CGC^{AG}GCG 3′
3′ GCG$_{AG}$CG 5′ 3′ GCG$_{GA}$CG 5′ 3′ CCG$_{AG}$CGG 5′ 3′ GCG$_{GA}$CGC 5′

Henceforth, nucleotides within internal loops are underlined. Thermodynamic parameters for related sequences with functional group substitutions are listed in Tables I and II. The parameters were derived from fits of melting curves and from T_M^{-1} vs log C_T plots. Plots of T_M^{-1} vs log C_T are shown in Figure 2 and in supplementary material. Except for rGCPGGCG, the parameters derived from the two methods agree within 10%. This suggests the bimolecular, two-state model is a reasonable approximation for these transitions.[17,18]

As shown in Figure 3, the melting profile for rGCPGGCG is not two-state; a biphasic transition is observed for oligomer concentrations greater than 0.1 mM. For this case, the data were truncated at the start of the second transition and fit with the two-state algorithm. The $\Delta G°_{37}$, $\Delta H°$, and $\Delta S°$ derived from the fitted data for the lower transition of rGCPGGCG are similar to those obtained for rGCGPGCG. The $\Delta H°$ and $\Delta S°$ obtained from the T_M^{-1} vs log C_T plot are more than 30% larger than the results obtained by averaging the fitted data. Thus, the results for rGCPGGCG must be treated with some caution. The melting profile for rCGCPGGCG, however, is monophasic below 0.5 mM

(12) Gralla, J.; Crothers, D. M. *J. Mol. Biol.* **1983**, *78*, 301–319.
(13) Jaeger, J. A.; Turner, D. H.; Zuker, M. *Proc. Natl. Acad. Sci. U.S.A.* **1989**, *86*, 7706–7710.
(14) SantaLucia, J., Jr.; Kierzek, R.; Turner, D. H. *Biochemistry* **1990**, *29*, 8813–8819.
(15) Kierzek, R.; Caruthers, M. H.; Longfellow, C. E.; Swinton, D.; Turner, D. H.; Freier, S. M. *Biochemistry* **1986**, *25*, 7840–7846.
(16) Markiewicz, W. T.; Biala, E.; Kierzek, R. *Bull. Pol. Acad. Sci.* **1984**, *32*, 433–450.
(17) Freier, S. M.; Burger, B. J.; Alkema, D.; Neilson, T.; Turner, D. H. *Biochemistry* **1983**, *22*, 6198–6206.
(18) Petersheim, M.; Turner, D. H. *Biochemistry* **1983**, *22*, 256–263.

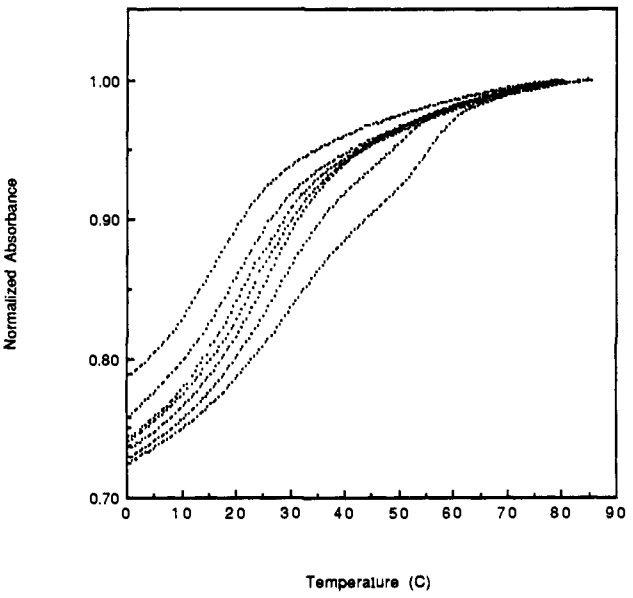

Figure 3. Normalized absorbance curves for rGCPGGCG. Note that higher concentration melts are biphasic.

(at 0.5 mM a small high melting transition is observed), and the T_M^{-1} vs log C_T data agree well with the fitted data, suggesting the rCGCPGGCG melting transition is two-state. Therefore, the results are more reliable for rCGCPGGCG than for rGCPGGCG.

Circular dichrosim (CD) spectra for the duplexes in 1 M Na^+ at 0 °C are shown in Figure 4 and in supplementary material. Oligomers with a G-A sequence in an internal loop have positive ellipticity in the 285-nm region[14] that is not observed for fully paired A-form RNA.[19] CD spectra for rGCGPGCG, rGCIAGCG, rGC2AGCG, and rGGCGPGCC retain this feature, suggesting that removing the amino group of adenine or the amino or O6 groups of guanine does not significantly affect the conformation of the helix. CD spectra of sequences with terminal GA and GP sequences are similar to each other. CD spectra of rAGCGCGA, rAGCGCGP, and rPGCGCGP are also similar to each other (see supplementary material). These results suggest the structure of external mismatches and 3'-dangling ends are also not significantly affected by removal of adenine's amino group.

Oligomers with an A-G sequence in an internal loop have a small negative band near 280 nm and spectra that are similar to those expected for A-form RNA.[14] The CD spectrum for rGCPGGCG, however, has positive ellipticity at 280 nm, suggesting removal of adenine's amino group in this context does affect the duplex structure.

Discussion

The interactions determining stabilities and structures of internal loops in RNA are not well understood. A recent study indicated that internal loops with GA mismatches are more stable than internal loops with AA mismatches.[14] At the termini of RNA duplexes, however, GA and AA mismatches have similar stabilities.[11] Since GA mismatches are known to form a variety of hydrogen-bonded structures in DNA,[20-25] this suggests hydrogen bonding may be more important for internal mismatches than for external mismatches. Therefore, we have determined the thermodynamic contribution of specific hydrogen-bonding groups to the stability of internal and external mismatches by making functional group substitutions.

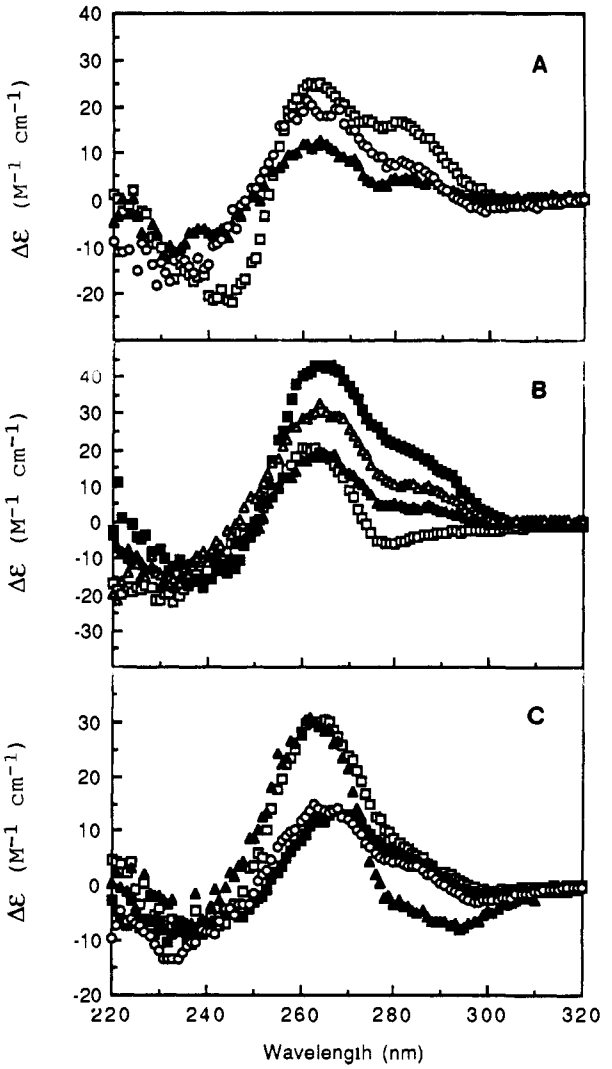

Figure 4. CD spectra at 0 °C for (A) rGCGAGCG (□), GCGPGCG (▲), and rGCIAGCG (○); (B) rGCAGGCG (□), rGCPGGCG (▲), rGGCGAGCC (■), and rGGCGPGCC (△); and (C) rGAGCGCGA (□), rGPGCGCGP (▲), rAGCGCG (■), and rPGCGCG (○).

To our knowledge, this paper presents the first chemical incorporation of purine riboside into oligoribonucleotides. Synthesis of 9-(2'-*O*-tetrahydropyranyl-5'-*O*-(dimethoxytrityl)-β-D-ribofuranosyl)purine was done by analogy to the procedure for uridine described by Markiewicz et al.[16] Synthesis of the 2-aminopurine blocked monomer, 2-isobutyramido-9-(2'-*O*-tetrahydropyranyl-5'-*O*-(dimethoxytrityl)-β-D-ribofuranosyl)purine, required transformation of the guanine base to 2-aminopurine[26] following proper protection of the riboside moiety.[16] The protected nucleosides were then converted to 3'-*O*-phosphoramidites and incorporated into oligonucleotides.[15] This demonstrates that the methodology described by Kierzek et al.[15] is general and allows incorporation of analogues of the natural nucleosides into oligoribonucleotides.

After this paper was submitted, an alternate route to oligoribonucleotides containing 2-aminopurine was reported.[27] This route uses the method of Fox et al.[28] to generate 2-aminopurine

(19) Tunis-Schneider, M. J. B.; Maestre, M. F. *J. Mol. Biol.* **1970**, *52*, 521-541.
(20) Brown, T.; Hunter, W. H.; Kneale, G.; Kennard, O. *Proc. Natl. Acad. Sci. U.S.A.* **1986**, *83*, 2402-2406.
(21) Gao, X.; Patel, D. J. *J. Am. Chem. Soc.* **1988**, *110*, 5178-5182.
(22) Kan, L.-S.; Chandrasegaran, S.; Pulford, S. M.; Miller, P. S. *Proc. Natl. Acad. Sci. U.S.A.* **1983**, *80*, 4263-4265.
(23) Li, Y.; Zon, G.; Wilson, W. D. *Proc. Natl. Acad. Sci. U.S.A.* **1991**, *88*, 26-30.
(24) Prive, G.; Heinemann, U.; Chandrasegaran, S.; Kan, L.-S.; Kopka, M. L.; Dickerson, R. E. *Science* **1987**, *238*, 498-504.
(25) Wilson, W. D.; Hoa, D. T. M.; Zuo, E. T.; Zon, G. *Nucleic Acids Res.* **1988**, *16*, 5137-5151.
(26) McLaughlin, L. W.; Leong, T. Benseler, F.; Piel, N. *Nucleic Acids Res.* **1988**, *16*, 5631-5644.
(27) Doudna, J. A.; Szostak, J. W.; Rich, A.; Usman, N. *J. Org. Chem.* **1990**, *55*, 5547-5549.

Table I. Thermodynamic Parameters of Duplex Formation for Helixes with Internal Loops[a]

RNA duplex	$1/T_M$ vs log C_T parameters				curve fit parameters		
	$-\Delta G°_{37}$, kcal/mol	$-\Delta H°$, kcal/mol	$-\Delta s°$, eu	T_M,[b] °C	$-\Delta G°_{37}$, kcal/mol	$-\Delta H°$, kcal/mol	$-\Delta S°$, eu
$\frac{GC^{GA}GCG}{GCG_{AG}CG}$[c]	6.68 ± 0.21	55.0 ± 4.5	155.8 ± 7.7	42.8	6.73 ± 0.12	55.9 ± 3.3	158.6 ± 10.6
$\frac{GC^{GP}GCG}{GCG_{PG}CG}$	3.89 ± 0.10	42.3 ± 1.0	123.9 ± 3.2	24.5	3.84 ± 0.18	43.2 ± 1.6	127.0 ± 5.8
$\frac{GC^{IA}GCG}{GCG_{AI}CG}$	7.46 ± 0.23	61.0 ± 2.7	172.7 ± 8.2	46.4	7.57 ± 0.11	64.1 ± 1.3	182.4 ± 3.9
$\frac{GC^{IP}GCG}{GCG_{PI}CG}$	4.26 ± 0.07	48.2 ± 0.8	141.8 ± 2.8	28.2	4.30 ± 0.09	48.0 ± 2.2	141.0 ± 7.5
$\frac{GC^{PP}GCG}{GCG_{PP}CG}$	3.12 ± 0.06	48.4 ± 0.7	146.0 ± 2.4	21.5	3.43 ± 0.12	43.1 ± 1.5	128.0 ± 4.9
$\frac{GC^{AA}GCG}{GCG_{AA}CG}$[c]	4.19 ± 0.29	42.8 ± 2.9	124.4 ± 9.3	26.7	4.28 ± 0.19	41.4 ± 1.3	119.6 ± 4.4
$\frac{GC^{2A}GCG}{GCG_{A2}CG}$[e]	5.68 ± 0.13	52.0 ± 1.6	149.5 ± 5.2	37.1	5.72 ± 0.09	50.9 ± 2.0	145.6 ± 6.6
$\frac{GC^{AG}GCG}{GCG_{GA}CG}$[c]	6.32 ± 0.10	61.2 ± 1.3	176.9 ± 4.1	40.3	6.34 ± 0.05	60.4 ± 2.3	174.4 ± 7.5
$\frac{GC^{PG}GCG}{GCG_{GP}CG}$	3.16 ± 0.14	50.7 ± 1.7	153.2 ± 5.6	22.4	3.83 ± 0.14	38.1 ± 2.5	110.5 ± 8.0
$\frac{GC^{AI}GCG}{GCG_{IA}CG}$	7.51 ± 0.14	60.8 ± 1.7	171.9 ± 5.2	46.7	7.62 ± 0.14	63.6 ± 2.6	180.5 ± 7.9
$\frac{GGC^{GA}GCC}{CCG_{AG}CGG}$[c]	9.67 ± 0.24	66.0 ± 2.4	181.6 ± 7.2	57.0	10.16 ± 0.30	73.9 ± 3.9	205.6 ± 11.7
$\frac{GGC^{GA}GCC}{CCG_{AG}CGG}$[d]	9.26 ± 0.27	61.0 ± 2.4	166.9 ± 7.1	56.3	9.91 ± 0.34	72.6 ± 3.7	202.2 ± 11.0
$\frac{GGC^{GP}GCC}{CCG_{PG}CGG}$	6.70 ± 0.08	56.7 ± 1.1	161.1 ± 3.3	42.8	6.80 ± 0.11	60.5 ± 3.6	173.1 ± 11.5
$\frac{CGC^{AA}GCG}{GCG_{AA}CGC}$[f]	5.43 ± 0.07	48.0 ± 1.1	137.1 ± 3.5	35.5	5.59 ± 0.22	40.1 ± 4.1	111.3 ± 13.7
$\frac{CGC^{AG}GCG}{GCG_{GA}CGC}$[c]	7.75 ± 0.22	60.3 ± 2.6	169.4 ± 7.9	48.1	7.90 ± 0.13	65.5 ± 2.8	185.6 ± 8.9
$\frac{CGC^{PG}GCG}{GCG_{GP}CGC}$	5.07 ± 0.12	56.6 ± 1.6	166.2 ± 5.2	33.6	5.11 ± 0.07	55.3 ± 1.2	161.8 ± 4.1
$\frac{CGC^{AI}GCG}{GCG_{IA}CGC}$	9.11 ± 0.17	67.8 ± 1.9	189.4 ± 5.8	53.6	9.33 ± 0.22	71.9 ± 3.4	201.9 ± 10.3
reference duplexes							
$\frac{GCGCGp}{pGCGCG}$[g]	7.64 ± 0.08	46.8 ± 0.9	126.3 ± 2.8	50.7	7.76 ± 0.17	48.8 ± 1.9	132.5 ± 5.5
$\frac{GGCGCCp}{pCCGCGG}$[g]	11.31 ± 0.05	67.7 ± 0.5	181.8 ± 1.4	65.2	10.99 ± 0.12	63.4 ± 1.8	169.1 ± 5.4
$\frac{CGCGCGp}{pGCGCGC}$[g]	9.11 ± 0.05	54.4 ± 0.5	146.2 ± 1.6	57.9	9.06 ± 0.14	53.1 ± 2.0	142.1 ± 6.1

[a] Solutions are 1 M NaCl, 10 mM sodium cacodylate, 0.5 mM Na_2EDTA, pH 7. [b] Calculated for 10^{-4} M oligomer concentration. [c] Reference 14. [d] Solution is 1 M NaCl, 50 mM morpholinoethanesulfonic acid, 0.5 mM Na_2EDTA, pH 5.5. [e] 2 = 2-aminopurine. [f] Sugimoto, N.; Kierzek, R.; Turner, D. H. Unpublished results. [g] Reference 45.

and the method of Usman et al.[29] for blocking the 2′ OH with *tert*-butyldimethylsilyl (TBDMSi). Protection with silyl has the advantage that the blocking group is not acid labile. Thus, all the 2′ OH groups remain blocked during the acid detritylation required prior to each addition of monomer to oligoribonucleotide. This allows synthesis of long chains.[29] The disadvantage of silyl is that deprotection requires several additional steps. For the synthesis of octamers, we obtain similar final yields with TBDMSi or tetrahydropyranyl protection. Evidently, for synthesis of short oligomers, the ease of deprotection with tetrahydropyranyl compensates for the partial loss of 2′ OH protection.[15]

For all sequences, the melting temperatures of the oligomers are concentration dependent. This indicates that any potential structures with hairpin loops are less stable than structures of higher molecularity, since T_M's of unimolecular hairpins are independent of concentration. The good agreement between parameters derived from fits of individual melting curves and from T_M^{-1} vs log C_T plots by using a bimolecular two-state model indicates the oligomers are forming duplexes.[14] The stabilities of the internal loops of the duplexes can be calculated from equations analogous to[12] $\Delta G°_{37,\text{loop}} = \Delta G°_{37}(\text{rGCGAGCG}) - \Delta G°_{37}(\text{rGCGCG}) + \Delta G°_{37}(\frac{CG}{GC})$. $\Delta G°_{37}(\frac{CG}{GC})$ is the free energy increment for the nearest neighbor base pair interaction[30] inter-

(28) Fox, J. J.; Wempen, I.; Hampton, A.; Doerr, I. L. *J. Am. Chem. Soc.* **1958**, *80*, 1669–1672.
(29) Usman, N.; Ogilvie, K. K.; Jiang, M. Y.; Cedergen, R. L. *J. Am. Chem. Soc.* **1987**, *109*, 7845–7854.
(30) Freier, S. M.; Kierzek, R.; Jaeger, J. A.; Sugimoto, N.; Caruthers, M. H.; Neilson, T.; Turner, D. H. *Proc. Natl. Acad. Sci. U.S.A.* **1986**, *83*, 9373–9377.

Table II. Thermodynamic Parameters of Duplex Formation for Helixes with Terminal Mismatches[a]

RNA duplex	$1/T_M$ vs log C_T parameters				curve fit parameters		
	$-\Delta G°_{37}$, kcal/mol	$-\Delta H°$, kcal/mol	$-\Delta S°$, eu	T_M,[b] °C	$-\Delta/G°_{37}$, kcal/mol	$-\Delta H°$, kcal/mol	$-\Delta S°$, eu
AGCGCG GCGCGA	7.43 ± 0.05	46.8 ± 0.4	126.8 ± 1.4	49.1	7.41 ± 0.05	45.3 ± 1.5	122.1 ± 4.9
PGCGCG GCGCGP	7.35 ± 0.12	44.5 ± 1.1	119.9 ± 3.4	49.2	7.39 ± 0.08	45.0 ± 0.8	121.4 ± 2.4
AGCGCGA AGCGCGA	8.54 ± 0.15	48.4 ± 1.2	128.7 ± 3.4	56.5	8.69 ± 0.11	51.2 ± 1.0	137.0 ± 3.1
AGCGCGP PGCGCGA	8.71 ± 0.10	51.0 ± 0.8	136.3 ± 2.4	56.7	8.81 ± 0.04	53.0 ± 1.3	142.4 ± 4.2
PGCGCGP PGCGCGP	8.27 ± 0.15	49.2 ± 1.3	132.0 ± 4.0	54.3	8.35 ± 0.08	50.7 ± 0.9	136.6 ± 3.0
GAGCGCGA AGCGCGAG	9.41 ± 0.13	56.3 ± 1.2	151.3 ± 3.4	59.1	9.44 ± 0.10	56.8 ± 1.7	152.7 ± 5.3
GPGCGCGP PGCGCGPG	8.81 ± 0.19	52.5 ± 1.8	140.8 ± 5.3	56.7	8.75 ± 0.11	51.0 ± 1.2	136.2 ± 3.8
GCCGGAp[c,d] pAGGCCG	7.05 ± 0.06	45.3 ± 0.8	123.2 ± 2.4	46.7	7.30 ± 0.25	49.1 ± 6.3	134.6 ± 19.6
GCCGGAG[c] GAGGCCG	8.45 ± 0.15	54.9 ± 1.5	149.8 ± 4.4	53.6	8.52 ± 0.11	56.5 ± 2.8	154.6 ± 8.9
reference duplexes							
GCGC[c,d] CGCG	4.61 ± 0.03	30.4 ± 0.3	83.3 ± 0.8	26.5	4.68 ± 0.12	34.0 ± 6.0	94.6 ± 19.2
CCGG[e] GGCC	4.36 ± 0.1	34.2 ± 0.2	95.6 ± 0.8	27.1	4.41 ± 0.1	34.7 ± 3.0	97.1 ± 10.0

[a] Solutions are 1 M NaCl, 10 mM sodium cacodylate, 0.5 mM Na_2EDTA, pH 7. [b] Calculated for 10^{-4} M oligomer concentration. [c] Solutions are 1 M NaCl, 10 mM sodium phosphate, and 0.5 mM Na_2EDTA, pH 7. [d] Reference 45. [e] Reference 18.

Table III. Thermodynamic Parameters of Loop and End Formation[a]

RNA sequence	$\Delta G°_{37}$, kcal/mol	$\Delta H°$, kcal/mol	$\Delta S°$, eu
	Loop Parameters		
GCGAGCG	−1.04 ± 0.23	−16.2 ± 4.7	−48.9 ± 8.5
GCGPGCG	1.75 ± 0.14	−3.5 ± 1.6	−17.0 ± 4.9
GC2AGCG	0.04 ± 0.16	−13.2 ± 2.0	−42.6 ± 6.4
GCIAGCG	−1.82 ± 0.25	−22.2 ± 3.0	−65.8 ± 9.0
GCIPGCG	1.38 ± 0.12	−9.5 ± 1.5	−34.9 ± 4.6
GCPPGCG	2.52 ± 0.12	−9.6 ± 1.4	−39.1 ± 4.4
GCAAGCG	1.45 ± 0.31	−4.0 ± 3.1	−17.5 ± 10.0
GCAGGCG	−0.68 ± 0.14	−22.4 ± 1.8	−70.0 ± 5.5
GCPGGCG	2.48 ± 0.17	−11.9 ± 2.1	−46.3 ± 6.7
GCAIGCG	−1.87 ± 0.17	−22.0 ± 2.1	−65.0 ± 6.4
GGCGAGCC	−0.36 ± 0.28	−6.3 ± 2.6	−19.2 ± 7.7
GGCGPGCC	2.61 ± 0.11	3.0 ± 1.5	1.3 ± 4.3
CGCAAGCG	1.68 ± 0.11	−1.6 ± 1.5	−10.3 ± 4.5
CGCAGGCG	−0.64 ± 0.23	−13.9 ± 2.8	−42.6 ± 8.4
CGCPGGCG	2.04 ± 0.14	−10.2 ± 1.9	−39.4 ± 5.9
CGCAIGCG	−2.00 ± 0.19	−21.5 ± 2.1	−62.6 ± 6.5
	End Parameters		
AGCGCG	−1.41 ± 0.03	−8.2 ± 0.3	−21.8 ± 0.8
PGCGCG	−1.37 ± 0.06	−7.1 ± 0.6	−18.3 ± 1.8
AGCGCGA	−1.97 ± 0.08	−9.0 ± 0.6	−22.7 ± 1.8
AGCGCGP	−2.05 ± 0.05	−10.3 ± 0.4	−26.5 ± 1.3
PGCGCGP	−1.83 ± 0.10	−9.4 ± 0.7	−24.4 ± 2.0
AGCGCGA	−0.56 ± 0.08	−0.8 ± 0.6	−1.0 ± 1.8
AGCGCGP	−0.64 ± 0.06	−2.1 ± 0.5	−4.8 ± 1.4
PGCGCGP	−0.46 ± 0.08	−2.4 ± 0.9	−6.1 ± 2.6
GAGCGCGA	−2.40 ± 0.07	−13.0 ± 0.6	−34.0 ± 1.8
GPGCGCGP	−2.10 ± 0.10	−11.1 ± 0.9	−28.8 ± 2.7
GAGCGCGA	−0.99 ± 0.07	−4.8 ± 0.6	−12.3 ± 1.8
GPGCGCGP	−0.73 ± 0.11	−4.0 ± 1.1	−10.5 ± 3.2
GCCGGAp	−1.35 ± 0.06	−5.6 ± 0.4	−13.8 ± 1.3
GCCGGAG	−2.05 ± 0.09	−10.4 ± 0.8	−27.1 ± 2.2
GCCGGAG	−0.70 ± 0.08	−4.8 ± 0.9	−13.3 ± 2.5

[a] Calculated from T_M^{-1} vs log C_T parameters.

rupted by the internal loop. The results are listed in Table III.

To determine the contributions of specific functional groups to stabilities of the internal loops, the following substitutions were made: A→P, i.e. replacement of the amino group of A with hydrogen; G→I, i.e. replacement of the amino group of G with hydrogen; and G→2, i.e. replacement of the O6 of G with hydrogen coupled with deletion of the imino proton (see Figure 1). The largest change is induced by the A→P substitution. For both G-A and A-G internal loops, this reduces loop stability by at least 2.7 kcal/mol, or about −1.4 kcal/mol mismatch. Presumably, this reflects hydrogen bonding, e.g. $\Delta G°_{\text{H-bonding}} = 0.5[\Delta G°(\text{rGCGAGCG}) - \Delta G°(\text{rGCGPGCG})]$. Results of similar calculations for other sequences and functional groups are listed in Table IV.

Table IV. Thermodynamic Parameters of Hydrogen Bond Formation[a]

RNA sequence	$\Delta G°_{37}$, kcal/mol	$\Delta H°$, kcal/mol	$\Delta S°$, eu
GCGAGCG	−1.39 ± 0.12	−6.4 ± 1.3	−16.0 ± 4.2
GCAGGCG	−1.58 ± 0.09	−5.3 ± 1.1	−11.8 ± 3.5
GGCGAGCC	−1.48 ± 0.14	−4.7 ± 1.3	−10.3 ± 4.0
CGCAGGCG	−1.34 ± 0.13	−1.9 ± 1.5	−1.6 ± 4.7
GCIAGCG	−1.60 ± 0.12	−6.4 ± 1.4	−15.4 ± 4.3
GC(G-I)AGCG	0.39 ± 0.16	3.0 ± 1.8	8.4 ± 5.6
GCA(G-I)GCG	0.59 ± 0.09	−0.2 ± 1.1	−2.5 ± 3.3
CGCA(G-I)GCG	0.68 ± 0.14	3.8 ± 1.6	10.0 ± 4.9
GCAAGCG	−0.27 ± 0.07	1.4 ± 0.7	5.4 ± 2.4
AGCGCG	−0.04 ± 0.07	−1.1 ± 0.6	−3.5 ± 1.9
AGCGCGP	−0.22 ± 0.09	−0.9 ± 0.8	−2.2 ± 2.4
GAGCGCGA	−0.15 ± 0.06	−1.0 ± 0.5	−2.6 ± 1.6

[a] Calculated from T_M^{-1} vs log C_T parameters. For sequences without (G-I), the values are the change in duplex stability upon substituting purine for each underlined A, divided by 2 times the number of A's substituted, e.g. $\Delta G°_{\text{H-bonding}} = 0.5[\Delta G°(\text{rGCGAGCG}) - \Delta G°(\text{rGCGPGCG})]$. For sequences with (G-I), the values are half the change in duplex stability upon substituting inosine for the underlined G.

Interestingly, the adenine group forms hydrogen bonds with similar thermodynamic parameters whether the order of the GA mismatches is G-A or A-G. This contrasts with the structural differences of G-A vs A-G reported previously.[14] In that study, an NMR resonance at 11.98 ppm with a line width of about 11 Hz was assigned to the imino protons of the GA mismatches in CGCAGGCG. Furthermore, an NOE from the G imino to the A-H2 indicates the GA mismatches in rCGCAGGCG form the structure shown at the top of Figure 1. No corresponding resonance was observed for rGGCGAGCC from 11 to 14 ppm. Recently, however, we have observed a previously unreported

G(anti) - A(anti)

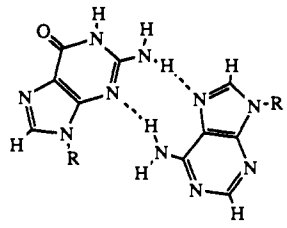

G(anti) - A(syn)

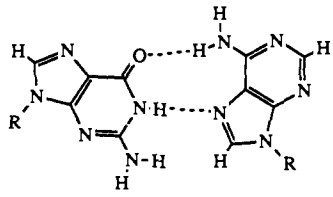

G(syn) - A(anti,H^+)

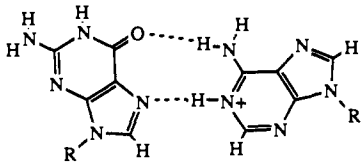

Figure 5. Proposed GA mismatch structures (top to bottom): G-(anti)-A(anti,Hoogsteen), proposed by Li, Wilson, and Zon; G(anti)-A-(syn,Hoogsteen); G(syn,Hoogsteen)-A(anti,H+).

resonance for rGGCGAGCC at 10.1 ppm with a line width of about 100 Hz. This suggests A-G sequences involve hydrogen-bonded imino protons, whereas G-A sequences do not. Potential hydrogen bonding configurations for GA mismatches are shown in Figures 1 (top) and 5. The thermodynamic results for rGGCGAGCC measured at pH 7.0 and 5.5 are the same within experimental error (see Table I), suggesting the G(syn)-A(anti,H^+) structure (see Figure 5 (bottom)) is not formed.

One ambiguity with using functional group substitutions to evaluate hydrogen bonding between nucleic acid bases is that each functional group is electronically coupled via the aromatic ring π electrons to other potential hydrogen bond acceptor or donor sites. This effect can be qualitatively examined by comparing pK_a's for various sites on mononucleosides. For example, the pK_a of adenosine N1 is 3.5, but the pK_a of purine riboside N1 is 2.1 (see Figure 6).[31] This suggests that adenosine N1 is a better hydrogen bond acceptor than purine riboside. Thus removing the amino group of A also affects hydrogen bonds to N1. Theoretical calculations of charge densities at adenine N1 vs purine N1 also suggest adenine is a better hydrogen bond acceptor.[32,33] Removal of a single functional group also removes any resonance stabilization energy from formation of two hydrogen bonds within the π electron system.[34-36] Therefore, the −1.4-kcal/mol difference

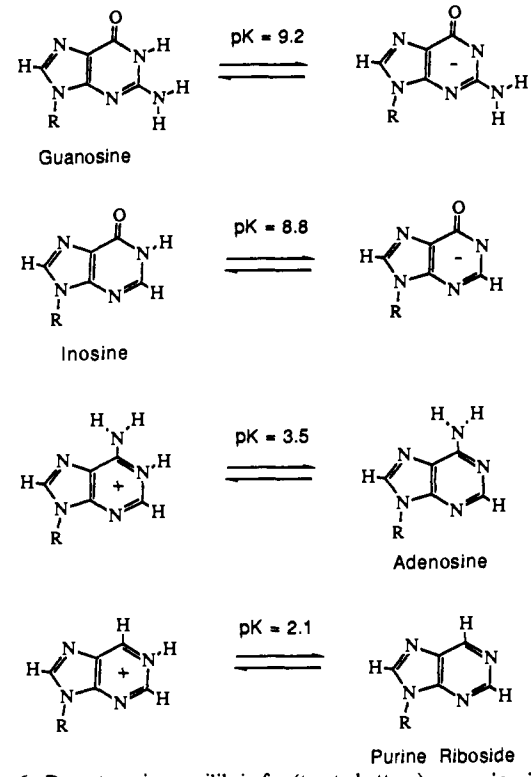

Figure 6. Deprotonation equilibria for (top to bottom) guanosine, inosine, adenosine, and purine riboside.

in stability between GA and GP mismatches represents a lower limit for total hydrogen bonding from the N1 and NH_2 positions. It is possible, however, that for G-A sequences the difference largely reflects interactions involving the NH_2 group, since no NMR resonance is observed for an imino proton hydrogen bonding to N1.[14]

Another potential ambiguity with functional group substitutions or deletions is that removal of functional groups may affect stacking. Theoretical studies have shown that stacking energy is predominantly due to induced dipole–induced dipole (van der Waals) interactions, suggesting the details of electronic structure are not very important for stacking.[32,37,38] This is consistent with experimental data for stabilization of duplexes by unpaired dangling end nucleotides. For example, A, G, ϵA, and I all add similar free energy and enthalpy increments as dangling ends.[8,17] To determine if adenine and purine stack similarly, stabilities were measured for duplexes with either A or P as 3'-dangling ends on terminal GA or GP mismatches. As shown in Table II, substitution of A with P had little effect. For example, rAGCGCGA and rAGCGCGP duplexes have the same $\Delta G°$, $\Delta H°$, $\Delta S°$, and T_M within experimental error. Furthermore, CD spectra for the two molecules are similar (see supplementary material), suggesting that removal of adenine's amino group also does not affect stacking geometry. As a further control, the consequences of removing adenine amino groups in the interior of the duplex were investigated. Table I gives the results for the sequences rGCAAGCG and rGCPPGCG. In this case, removal of four amino groups destabilizes the duplex by about 1.1 kcal/mol suggesting that each amino group contributes about 0.3 kcal/mol to duplex stability. This is a relatively small effect compared to the 1.4-kcal/mol decrease in stability observed for deleting an amino group in an internal GA mismatch. NMR studies of two deoxyoligonucleotide duplexes indicated the A to P substitution in AT base pairs also has no effect on conformation.[39,40]

(31) Richards, E. G. *Handbook of Biochemistry and Molecular Biology: Nucleic Acids*, 3rd ed.; Fasman, G. D., Ed.; CRC Press: Cleveland, OH, 1975; Vol. I.
(32) Pullman, A.; Pullman, B. *Adv. Quantum Chem.* **1986**, *4*, 267–325.
(33) Pullman, B.; Pullman, A. *Quantum Biochemistry*; Interscience: New York, 1963.
(34) Jorgensen, W. L.; Pranata, J. *J. Am. Chem. Soc.* **1990**, *112*, 2008–2010.
(35) Pauling, L. *The Nature of the Chemical Bond*; Cornell University Press: Ithaca, NY, 1960; Chapter 12.
(36) Saenger, W. *Principles of Nucleic Acid Structure*; Springer-Verlag: New York, 1984; Chapter 6.
(37) DeVoe, H.; Tinoco, I., Jr. *J. Mol. Biol.* **1962**, *4*, 500–517.
(38) Pullman, B.; Claverie, P.; Caillet, J. *Proc. Natl. Acad. Sci. U.S.A.* **1966**, *55*, 904–912.

As shown in Table III, the G to 2-aminopurine substitution decreases loop stability by about 0.5-kcal/mol mismatch. This modest effect is at first surprising since removal of the G O6 should eliminate the same hydrogen bond as removal of the A amino group. In this case, however, removal of the O6 is accompanied by removal of the imino proton. Thus a hydrogen bond donor is turned into a hydrogen bond acceptor. This makes the alternate structure shown in Figure 1 (bottom) possible. Thus the results for 2-aminopurine are also consistent with a hydrogen bond between the G carbonyl and A amino group. The thermodynamic consequences of eliminating this bond, however, are probably reduced by formation of different hydrogen bonds.

In contrast to the A amino group and G carbonyl group, removal of the 2-amino group of G (G→I) stabilizes each mismatch by about −0.5-kcal/mol mismatch (see Table I). This is not expected for the hydrogen bonding pattern observed for a GA mismatch in DNA by Li et al.[23] (see Figure 5, top), suggesting a different structure for the sequences studied here. The G→I substitution also stabilizes the mismatch with purine (see GCIPGCG in Table I). Evidently, removal of a hydrogen-bonding group that is not hydrogen bonded in the mismatch can be stabilizing. This may result from enhanced hydrogen bonding for the imino proton of I since the pK_a for I is 8.8 compared to 9.2 for G (see Figure 6). Alternate explanations are also possible. For example, the steric bulk of guanine's amino group or changes in solvation[41] may destabilize the duplex. These effects may explain why inosine is a better universal pairing base than guanosine in codon–anticodon interactions[41] and in hybridization.[42,43]

Replacement of the A amino group with hydrogen has the largest effect on the stabilities of the internal loops containing GA mismatches. The same substitution in GA mismatches at the termini of helixes, however, has almost no effect on stability. For example, substituting P for each A in $^{5'\ GAGCGCGA\ 3'}_{3'\ AGCGCGAG\ 5'}$ decreases duplex stability by only 0.6 kcal/mol or 0.15-kcal/mol mismatch. As shown by the results of related calculations listed in Table IV, this is the largest change observed for A→P substitutions at helix termini. Thus hydrogen bonding of the A amino group makes a negligible contribution to the stabilities of terminal GA mismatches.

The negligible effect observed for eliminating a potential hydrogen bond in a terminal GA mismatch contrasts with the significant effect observed for eliminating a hydrogen bond in a terminal GC pair.[8] When the terminal GC pairs in $(rCGGCCG)_2$ and $(rGCCGGC)_2$ are replaced with IC pairs, duplex stability decreases by 1.4 and 3.2 kcal/mol, respectively. Apparently, each terminal hydrogen bond involving the G amino group contributes −0.7 and −1.6 kcal/mol, respectively, to duplex stability. Similar changes in duplex stability have been observed in oligodeoxynucleotides when interior GC pairs are replaced with IC pairs.[43,44] Thermodynamic increments observed upon pairing of terminal bases also indicate substantial hydrogen bonding contributions to terminal base pair stability.[45] Moreover, stabilities measured for terminal and internal base pairs in oligoribonucleotides are the same within experimental error,[30,45] suggesting hydrogen bonding is similar for internal and external base pairs.

The above comparison suggests internal and external base pairs are similar, but internal and external purine–purine mismatches are different. One hypothesis consistent with the observations is that external purine–purine mismatches are conformationally free. Any functional groups that do not hydrogen bond within the duplex can hydrogen bond to water. Interior purine–purine mismatches, however, are conformationally restricted. Standard A-form geometry will produce steric clashes between the purines. Moreover, not every geometry will allow water to hydrogen bond to available functional groups. In this context, hydrogen bonding between functional groups within an interior mismatch can provide a favorable interaction not otherwise available.

The results of this work have important implications for prediction of RNA structure from sequence. Due to lack of experimental data, most algorithms for structure prediction assume the stability of an internal loop is independent of sequence in the loop.[12,46,47] The results in Table III show that the free energy increment for an internal loop at 37 °C can change by more than 4 kcal/mol depending on the sequence in the loop. Recently, Jaeger et al.[13] have suggested the sequence dependence of internal loop stability may be approximated by free energy increments measured for terminal mismatches. The results in Table III indicate this is also oversimplified. Terminal GA and GP mismatches have similar free energy increments as terminal mismatches, but internal loops with two GA or GP mismatches differ in stability by about 3 kcal/mol. Evidently, it will be necessary to add hydrogen bonding effects to approximations for internal loop stability.

The results in Tables II and III also provide additional insight into interactions at the ends of RNA helixes. The free energy increment for a terminal $^{CG}_{GA}$ nearest neighbor is measured for the first time. It is −1.4-kcal/mol mismatch, significantly less favorable than the previously approximated value of −1.9 kcal/mol.[11,30] This suggests the stabilities of terminal mismatches on CG pairs may be less favorable than thought. Free energy increments for adding terminal mismatches or single unpaired nucleotides adjacent to a mismatch are also measured for the first time, and range from −0.5 to −1 kcal/mol (see end parameters in Table III). These increments are neglected in current algorithms for prediction of RNA structure.

Experimental Section

General Materials and Methods. Anhydrous hydrazine, 3,4-dihydro-2*H*-pyran (DHP), 4,4′-dimethoxytrityl chloride (DMTr-Cl), 1,3-dichloro-1,1,3,3-tetraisopropyldisiloxane, *p*-toluenesulfonic acid monohydrate (p-TSA), and 2,4,6-triisopropylbenzenesulfonyl chloride (TPS-Cl) were from Aldrich and used without further purification. Nebularine (purine riboside) was purchased from Sigma. Thin-layer chromatography (TLC) was performed with 3 × 13 cm silica gel 250-μm layer F60 glass plates (Baker) with the following eluents: chloroform/methanol 9:1 (v/v) (system A); chloroform/methanol 95:5 (v/v) (system B); acetone/hexane/triethylamine 45:45:10 (v/v) (system C). Reverse-phase TLC was performed with 3 × 13 cm silica gel RP-8 F254s (E.M. Science) eluting with acetone/water 7:3 (v/v) (system D). Nucleoside derivatives were visualized by UV absorbance or by observing released trityl cation upon heating. Column chromatography was performed with silica gel 60H from Merck.

^1H and ^{31}P nuclear magnetic resonance (NMR) spectra were obtained on Varian VXR-500S and General Electric QE-300 spectrometers. ^1H NMR spectra were referenced to internal $CHCl_3$ (δ 7.24 ppm). ^{31}P NMR chemical shifts were referenced to external 1% phosphoric acid, and CD_3CN (MSD Isotopes) was used as lock reference. Ultraviolet (UV) spectra were recorded in methanol on a Perkin-Elmer 330 spectrophotometer. Fluorescence spectra were recorded on a Perkin-Elmer MPF-44A spectrofluorimeter.

Synthesis of Blocked Monomers. The syntheses of blocked adenosine, cytidine, guanosine, and uracil have been described in detail.[16] The synthesis of blocked inosine is similar to that described for uridine.

Blocked Purine Riboside. Since purine has no exocyclic amino group to protect, the protection scheme chosen is similar to that described for uridine.[16]

9-(3′,5′-*O*-Tetraisopropyldisiloxane-1,3-diyl-β-D-ribofuranosyl)purine (1). To 1.75 g (6.9 mmol) of nebularine was added 20 mL of dry

(39) Clore, G. M.; Oshkinat, H.; McLaughlin, L. W.; Benseler, F.; Happ, C. S.; Happ, E.; Gronenborn, A. M. *Biochemistry* **1988**, *27*, 4185–5197.
(40) Ikuta, S.; Eritja, R.; Kaplan, B. E.; Itakura, K. *Biochemistry* **1987**, *26*, 5646–5650.
(41) Crick, F. H. C. *J. Mol. Biol.* **1966**, *19*, 548–555.
(42) Martin, F. H.; Castro, M. M.; Aboul-ela, F.; Tinoco, I., Jr. *Nucleic Acids Res.* **1985**, *13*, 8927.
(43) Kawase, Y.; Iwai, S.; Inoue, H.; Miura, K.; Ohtsuka, E. *Nucleic Acids Res.* **1986**, *14*, 7727–7736.
(44) Aboul-ela, F.; Koh, D.; Tinoco, I., Jr.; Martin, F. H. *Nucleic Acids Res.* **1985**, *13*, 4811–4824.
(45) Freier, S. M.; Sugimoto, N.; Sinclair, A.; Alkema, D.; Neilson, T.; Kierzek, R.; Caruthers, M. H.; Turner, D. H. *Biochemistry* **1986**, *25*, 3214–3219.
(46) Salser, W. *Cold Spring Harbor Symp. Quant. Biol.* **1977**, *42*, 985–1002.
(47) Tinoco, I., Jr.; Borer, P. N.; Dengler, B.; Levine, M. D.; Uhlenbeck, O. C.; Crothers, D. M.; Gralla, J. *Nature (London), New Biol.* **1973**, *246*, 40–41.

pyridine, and the solution was evaporated to dryness (2×) to remove traces of water. To the dry residue were added 14 mL of dry pyridine and 2.68 mL (8.5 mmol) of 1,3-dichloro-1,1,3,3-tetraisopropyldisiloxane, and the mixture was allowed to stir at ambient temperature for 2 h. The reaction was quenched by the addition of 10 mL of saturated sodium bicarbonate, and the product was extracted with chloroform and dried to an oil by rotary evaporation. ^{1}H NMR ($CDCl_3$, 300 MHz) δ (ppm) 9.2 (1 H, s, H-6), 8.9 (1 H, s, H-2), 8.3 (1 H, s, H-8), 6.1 (1 H, s, H-1'), 1.0–1.2 (28 H, m, isopropyl). UV λ_{min} 223 nm, λ_{sh} 250 nm, λ_{max} 261 nm. R_f (system A) 0.79; R_f (system B) 0.59.

9-(2′-*O*-Tetrahydropyranyl-3′,5′-*O*-tetraisopropyldisiloxane-1,3-diyl-β-D-ribofuranosyl)purine (2). Coevaporation of **1** with 50% toluene in chloroform was used to remove traces of pyridine. The crude reaction product was then dissolved in 22 mL of methylene chloride, and 3.4 mL (43.8 mmol) of DHP and 1.31 g (6.9 mmol) of pTSA (added in 0.2-g batches until a light pink color was observed) were added. The reaction was quenched after 12 h by adding 1.5 mL of triethylamine (TEA) and gave **2** as a mixture of diastereoisomers. The reaction mixture was dried to an oil by rotary evaporation and 10 mL dioxane was added and removed twice by rotary evaporation. ^{1}H NMR (mixture of diastereoisomers, $CDCl_3$, 300 MHz) δ (ppm) 9.2 (1 H, s, H-6), 8.5 (1 H, s, H-2), 8.4 (1 H, s, H-8), 6.2 (1 H, d, H-1'), 5.0 (1 H, t, tetrahydropyranyl (THP) H-2), 1.4–2.0 (8 H, M, THP), 0.8–1.1 (28 H, m, isopropyl). UV λ_{min} 223 nm, λ_{sh} 251 nm, λ_{max} 261 nm. R_f (system A) 0.88; R_f (system B) 0.75.

9-(2′-*O*-Tetrahydropyranyl-β-D-ribofuranosyl)purine (3). To the crude reaction product (**2**) was added 16 mL of 1 M triethylamine hydrofluoride (TEAHF) in tetrahydrofuran (THF)/dioxane, and the mixture was allowed to stir overnight. The reaction was quenched by the addition of saturated sodium bicarbonate and the product was extracted with chloroform and dried by rotary evaporation. The reaction gave **3** as a mixture of diastereoisomers. The product was then purified by column chromatography eluting with 2% methanol in chloroform. This purification produced better yields in the subsequent step. ^{1}H NMR (mixture of diastereoisomers, $CDCl_3$, 300 MHz) δ (ppm) 9.0 (1 H, 2 s, H-6), 8.8 (1 H, 2 s, H-2), 8.2 (1 H, 2 s, H-8), 5.9, 6.1 (1 H, 2 d, H-1'), 4.7, 4.9 (1 H, 2 t, THP H-2), 1.1–1.6 (8 H, m, THP). UV λ_{min} 222 nm, λ_{sh} 250 nm, λ_{max} 262 nm. R_f (system A) 0.40, 0.51.

9-(2′-*O*-Tetrahydropyranyl-5′-*O*-(dimethoxytrityl)-β-D-ribofuranosyl)purine (4). The purified product, **3**, was dissolved in 15 mL of pyridine and 2.34 g (6.9 mmol) of DMT-Cl was added and the mixture stirred for 2 h. The product was then worked up by extraction with satd. sodium bicarbonate/chloroform. Purification by column chromatography yielded 2.52 g of white amorphous solid as a mixture of diastereoisomers (58% isolated yield from nebularine). ^{1}H NMR (mixture of diastereoisomers, $CDCl_3$, 300 MHz) δ (ppm) 9.1 (1 H, 2 s, H-6), 8.9 (1 H, 2 s, H-2), 8.3 (1 H, 2 s, H-8), 6.7–7.5 (13 H, m, DMTr), 6.2, 6.3 (1 H, 2 d, H-1'), 5.0, 5.1 (1 H, 2 t, THP H-2), 3.8 (6 H, s, DMTr), 1.3–1.9 (8 H, m, THP). UV λ_{min} 253 nm, λ_{max} 262 nm, λ_{sh} 278 nm. R_f (system A) 0.76, 0.84; R_f (system C) 0.14, 0.22.

Blocked 2-Aminopurine Riboside. Blocked 2-aminopurine riboside was synthesized from guanosine by a method adapted from McLaughlin et al.[26]

2-*N*-Isobutyryl-2′,3′,5′-tri-*O*-isobutyrylguanosine (5). To 5.66 g (20 mmol) of guanosine in 160 mL of dry pyridine was added 26.6 mL (160 mmol) of isobutyric acid anhydride and 0.506 g (4 mmol) of 4-(*N*,*N*-dimethylamino)pyridine (DMAP). The mixture was stirred for 24 h at 50 °C. The reaction was quenched by adding 50 mL of methanol and worked up by extraction with saturated sodium bicarbonate/chloroform. ^{1}H NMR ($CDCl_3$, 500 MHz) δ (ppm) 12.1 (1 H, s, imino), 9.1 (1 H, s, 2-amido), 7.7 (1 H, s, H-8), 5.92 (1 H, d, J = 5.2 Hz, H-1'), 5.99 (1 H, t, J = 5.2 Hz, H2′ or H3′), 5.80 (1 H, t, J = 4.3 Hz, H2′ or H3′), 4.62 (1 H, m, H-4′ or H5′), 4.52 (2 H, m, H-4′, H5′, and/or H5″), 2.73 (1 H, m, J = 6.9 Hz, 2-isobutyramido, 2.50–2.65 (3 H, m, J = 6.9 Hz, 2′-, 3′-, 5′-isobutyryl), 1.1–1.4 (24 H, m, isobutyryl). UV λ_{min} 222 nm, 268 nm, λ_{max} 254 nm, 278 nm. R_f (system B) 0.73; R_f (system D) 0.35.

2-*N*-Isobutyryl-2′,3′,5′-tri-*O*-isobutyryl-6-*O*-(2,4,6-triisopropylbenzenesulfonyl)guanosine (6). The crude reaction product, **5**, was dissolved in 200 mL of chloroform and the following were added: 7.27 g (24 mmol) of TPS-Cl, 5.23 mL (30 mmol) of diisopropylethylamine, and 0.26 g (2 mmol) of DMAP. After 20 h the reaction was worked up by extraction with saturated sodium bicarbonate/chloroform. The product was purified by silica gel column chromatography using a gradient starting with hexane/chloroform (1:1) and ending with 100% chloroform. Upon evaporation of the solvent, 12.5 g of **6** was obtained as a solid white foam (86.5% yield). ^{1}H NMR ($CDCl_3$, 500 MHz) δ (ppm) 8.06 (1 H, s, 2-isobutyramido), 7.88 (1 H, s, H-8), 7.24 (2 H, s, TPS H-3, H-5), 6.14 (1 H, d, J = 4.2 Hz, H-1'), 5.80 (3 H, m, J = 5.4 Hz, TPS isopropyl), 2.94 (1 H, m, J = 6.9 Hz, 2-isobutyramido), 2.5–2.7 (3 H, m, J = 6.9 Hz, 2′-, 3′-, 5′-isobutyryl), 1.1–1.3 (42 H, m), isobutyryl, isopropyl). UV λ_{min} 265 nm, λ_{max} 224 nm, 278 nm, λ_{sh} 254 nm. R_f (system D) 0.17.

2-Isobutyramido-6-(2-isobutyrylhydrazino)-9-(2′,3′,5′-tri-*O*-isobutyryl-β-D-ribofuranosyl)purine (7). To 12.5 g (17.3 mmol) of the sulfonyl derivative, **6**, in 300 mL of dry dioxane cooled on ice was added dropwise with a syringe through a rubber septum 1.65 mL (51.9 mmol) of anhydrous hydrazine. After the addition was complete, the ice bath was removed and the mixture stirred 15 min at ambient temperature. TLC analysis showed that longer reaction times led to cleavage of the isobutyryl protection on the ribose ring. After reaction was complete, crude reaction product was worked up by extraction with saturated sodium bicarbonate/chloroform. R_f (system A) 0.33; R_f (system D) 0.40. After drying by rotary evaporation, the crude reaction product was immediately dissolved in 150 mL of chloroform, next 8.6 mL (51.9 mmol) of isobutyric acid anhydride, 0.214 g (1.7 mmol) of DMAP, and 7.3 mL (51.9 mmol) of TEA were added, and then the mixture was stirred for 30 min. After extraction with sodium bicarbonate/chloroform the product was purified by silica gel column chromatography (1–1.5% methanol in chloroform). This gave 8.20 g of **7** as a solid white foam (88% yield). ^{1}H NMR ($CDCl_3$, 300 MHz) δ (ppm) 8.02 (1 H, s, H-8), 6.10 (1 H, d, H-1'), 3.50 (1 H, m, isobutyramido), 2.9 (1 H, m, isobutyrylhydrazino), 2.5–2.7 (3 H, m, 2′-, 3′-, 5′-isobutyryl), 1.1–1.3 (30 H, m, isobutyryl). UV λ_{min} 248 nm, λ_{max} 226 nm, 275 nm, λ_{sh} 302 nm. R_f (system B) 0.84; R_f (system D) 0.29.

2-Isobutyramido-9-(2′,3′,5′-tri-*O*-isobutyryl-β-D-ribofuranosyl)purine (8). To 8.20 g (15.2 mmol) of **7** in 750 mL of dioxane/water (95:5 (v/v)) was added 17.3 g (75 mmol) of silver(I) oxide. The reaction mixture was vigorously stirred and heated under reflux at 110 °C for 24 h. The reaction mixture was filtered (Celite) and the solvents removed by rotary evaporation. The residue was dissolved in 500 mL of chloroform and washed three times with 500 mL of a 10% aqueous potassium iodide solution, three times with 500 mL of a 10% sodium thiosulfate solution, and twice with water, and dried by rotary evaporation. This gave 5.40 g of **8** as a solid white foam (81% yield). ^{1}H NMR ($CDCl_3$, 300 MHz) δ (ppm) 8.92 (1 H, s, H-6), 8.24 (1 H, s, 2-amido), 8.02 (1 H, s, H-8), 6.08 (1 H, d, H-1'), 2.75 (1 H, m, 2-isobutyramido), 2.4–2.6 (3 H, m, 2′-, 3′-, 5′-isobutyryl), 1.0–1.3 (24 H, m, isobutyryl). R_f (system B) 0.76; R_f (system D) 0.34.

2-Isobutyramido-9-β-D-ribofuranosylpurine (9). **8** (5.40 g, 12.3 mmol) was dissolved in 120 mL of methanol, the solution was cooled over an ice bath to ~5 °C, and 60 mL of a 1 M potassium hydroxide solution was added. After the mixture was stirred for 15 min, the reaction was stopped by adding ~50 g of Dowex 50WX8 (pyridinium form). The Dowex was filtered and washed with 100 mL of water/methanol (1:2 (v/v)). The filtrate was evaporated to give an oil. The oil was then partitioned between 50 mL of saturated sodium bicarbonate and 50 mL of chloroform (3×). The extracts were combined and evaporated to dryness to give a yellow foam. R_f (system A) 0.25; R_f (system D) 0.86.

2-Isobutyramido-9-(3′,5′-*O*-tetraisopropyldisiloxane-1,3-diyl-β-D-ribofuranosyl)purine (10). Subsequent protection of the ribose hydroxyl groups with DMTr and THP follows the procedure given in Markiewicz et al.[16] The crude reaction product, **9**, was dried by coevaporation with dry pyridine several times. The residue was dissolved in 30 mL of dry pyridine, 3.5 mL of 1,3-dichloro-1,1,3,3-tetraisopropyldisiloxane was added, and the mixture was stirred for 1 h. The product was washed with saturated sodium bicarbonate, extracted with chloroform, and dried by rotary evaporation. The product was purified by column chromatography (eluted with 2% methanol). This gave 3.70 g of **10** as a white solid foam (70% yield from **8**). ^{1}H NMR ($CDCl_3$, 500 MHz) δ (ppm) 8.9 (1 H, s, H-6), 8.35 (1 H, s, 2-amido), 8.25 (1 H, s, H-8), 6.08 (1 H, s, H-1'), 1.3 (6 H, d, isobutyryl), 1.0–1.2 (24 H, m, isopropyl). UV λ_{min} 242 nm, 266 nm, λ_{max} 255 nm, 285 nm. R_f (system B) 0.85; R_f (system D) 0.23.

2-Isobutyramido-9-(2′-*O*-tetrahydropyranyl-3′,5′-*O*-tetraisopropyldisiloxane-1,3-diyl-β-D-ribofuranosyl)purine (11). **10** (3.70 g, 8.5 mmol) was dissolved in 35 mL of methylene chloride and 3.85 mL (49.6 mmol) of DHP and 0.64 g (3.4 mmol) of pTSA were added. Reverse-phase TLC indicated the reaction was complete in 1 h. The reaction was quenched by adding 1.5 mL of TEA. The reaction product was worked up by extraction with saturated sodium bicarbonate/chloroform and dried by rotary evaporation to give **11** as a mixture of diastereoisomers. R_f (system B) 0.93; R_f (system D) 0.15 (diastereoisomers comigrate).

2-Isobutyramido-9-(2′-*O*-tetrahydropyranyl-β-D-ribofuranosyl)purine (12). Dioxane (30 mL) was added (2×) to **11** and removed by rotary evaporation. To the crude reaction product, 30 mL of 1 M TEAHF in THF/dioxane (1:1 (v/v)) was added and allowed to stir overnight. The reaction was quenched by the addition of saturated sodium bicarbonate, and the product was extracted with chloroform and dried by rotary evaporation to give **12** as a mixture of diastereoisomers. ^{1}H NMR (mixture of diastereoisomers, $CDCl_3$, 500 MHz) δ (ppm) 9.02, 8.99 (1 H, 2 s, H-6), 8.48, 8.39 (1 H, 2 s, H-8), 8.08 (1 H, 1 s, 2-amido), 6.03,

5.95 (1 H, 2 d, H-1'), 5.02, 4.95 (1 H, 2 t, THP H-2), 1.80–1.35 (8 H, m, THP), 1.32–1.28 (6 H, d, isobutyryl). UV λ_{min} 241 nm, 266 nm, λ_{max} 255 nm, 284 nm. R_f (system A) 0.36, 0.47; R_f (system D) 0.73.

2-Isobutyramido-9-(2'-*O*-tetrahydropyranyl-5'-*O*-(dimethoxytrityl)-β-D-ribofuranosyl)purine (13). The crude reaction product, **12**, was coevaporated with 10 mL of dry pyridine (3×) to remove traces of water and dissolved in 30 mL of pyridine, and then 3.04 g (9.0 mmol) of DMTr-Cl was added with stirring for 1 h. The product was then worked up by extraction with saturated sodium bicarbonate/chloroform. Purification by column chromatography and lyophylization from benzene yielded 2.7 g of white solid product (40% yield from **10**, 17% yield from guanosine). ^{1}H NMR larger R_f diastereoisomer ($CDCl_3$, 500 MHz) δ (ppm) 8.97 (1 H,.s, H-6), 8.16 (1 H, s, H-8), 7.82 (1 H, s, 2-amido), 7.2–7.5 (9 H, m, DMTr), 6.7–6.8 (4 H, m, DMTr), 6.13 (1 H, d, H-1'), 5.08 (1 H, t, THP H-2), 3.75 (6 H, s, DMTr), 1.4–1.9 (8 H, m, THP), 1.0–1.2 (6 H, d, isobutyryl). ^{1}H NMR smaller R_f diastereoisomer ($CDCl_3$, 500 MHz) δ (ppm) 8.97 (1 H, s, H-6), 8.12 (1 H, s, H-8), 7.82 (1 H, s, isobutyramido), 7.2–7.5 (9 H, m, DMTr), 6.7–6.8 (4 H, m, DMTr), 6.20 (1 H, d, H-1'), 5.20 (1 H, t, THP H-2), 1.4–1.9 (8 H, m, THP), 1.0–1.2 (6 H, d, isobutyryl). UV λ_{min} 266 nm, λ_{max} 282 nm. R_f (system A) 0.88, 0.92. R_f (system C) 0.54 broad; (system D) 0.35.

Preparation of Phosphoramidites. Phosphoramidites were prepared in situ as described by Kierzek et al.[15] This material was used without further purification for coupling reactions.

9-(2'-*O*-Tetrahydropyranyl-3'-*O*-[(diisopropylamino)(β-cyanoethoxy)phosphino]-5'-*O*-(dimethoxytrityl)-β-D-ribofuranosyl)purine (14). 4 (0.150 g, 0.24 mmol) and 0.020 g (0.12 mmol) of diisopropylammonium tetrazolide were dried in vacuo for 3 h followed by addition of anhydrous acetonitrile (1.2 mL) and bis(diisopropylamino)(β-cyanoethoxy)phosphine (Applied Biosystems) (0.076 g, 0.25 mmol). After 12 h, analysis by TLC indicated the reaction was complete. ^{31}P NMR (CD_3CN, 202.3 MHz) δ (ppm) 150.11, 150.16, 150.43, 150.47 (mixture of diastereoisomers). R_f (system C) 0.63.

2-Isobutyramido-9-(2'-*O*-tetrahydropyranyl-3'-*O*-[(diisopropylamino)(β-cyanoethoxy)phosphino]-5'-*O*-(dimethoxytrityl)-β-D-ribofuranosyl)purine (15). **13** (0.087 g, 0.12 mmol) and 0.010 g (0.06 mmol) of diisopropylammonium tetrazolide were dried in vacuo for 3 h followed by addition of anhydrous acetonitrile (0.6 mL) and bis(diisopropylamino)(β-cyanoethoxy)phosphine (0.036 g, 0.14 mmol). After 12 h, analysis by TLC indicated the reaction was complete. ^{31}P NMR (CD_3CN, 202.3 MHz) δ (ppm) 150.05, 150.08, 150.50, 150.54 (mixture of diastereoisomers). R_f (system C) 0.65.

9-(2'-*O*-Tetrahydropyranyl-3'-*O*-[(diisopropylamino)(β-cyanoethoxy)phosphino]-5'-*O*-(dimethoxytrityl)-β-D-ribofuranosyl)hypoxanthine (16). 9-(2'-*O*-Tetrahydropyranyl-5'-*O*-(dimethoxytrityl)-β-D-ribofuranosyl)hypoxanthine[8] (0.079 g, 0.12 mmol) and 0.010 g (0.06 mmol) of diisopropylammonium tetrazolide were dried in vacuo for 3 h followed by addition of anhydrous acetontrile (0.6 mL) and bis(diisopropylamino)(β-cyanoethoxy)phosphine (0.036 g, 0.14 mmol). After 12 h, analysis by TLC indicated the reaction was complete. ^{31}P NMR (CD_3CN, 202.3 MHz) δ (ppm) 149.89, 149.93, 150.13, 150.17 (mixture of diastereoisomers). R_f (system A) 0.54.

RNA Synthesis and Purification. Oligoribonucleotides were synthesized on solid support following a phosphoramidite approach.[15] After deblocking with ammonia, the crude mixture was purified by high-performance liquid chromatography (HPLC) on a PRP-1 semipreparative column (Hamilton) with a gradient of 0 to 50% acetonitrile buffered with 10 mM ammonium acetate, pH 7. Acid labile protecting groups were removed by treatment with 0.01 M HCl, pH 2.0, for 12 h. Sequences containing nebularine or 2-aminopurine riboside were further purified by preparative C-18 (Alltech) or C-8 (Beckman) HPLC. The RNA was desalted and further purified with a Sep-pak C-18 cartridge (Waters). Purities were checked by analytical C-8 (Beckman) HPLC and 500-MHz ^{1}H NMR at high temperature and were greater than 95%. The presence of 2-aminopurine in the sequence rGC2AGCG was verified by UV (λ_{max} = 252; 310 nm) and fluorescence spectrophotometry (uncorrected λ^{ex}_{max} = 310 nm; λ^{em}_{max} = 365 nm).

Melting Curves. The buffer for thermodynamic studies was 1.0 M NaCl, 10 mM sodium cacodylate, and 0.5 mM disodium ethylenediaminetetraacetate (Na_2EDTA), pH 7, unless otherwise noted. Strand concentrations were determined from high-temperature absorbance at 280 nm. Single strand extinction coefficients were calculated from extinction coefficients for dinucleoside monophosphates and nucleotides, as described previously.[31,48] The extinction coefficient for rGCGPGCG was determined by measuring the high-temperature absorbance at 280 nm, cleaving the RNA by treating with 1.0 M KOH at 70 °C overnight, and remeasuring the absorbance. C-8 HPLC was used to determine that full strand cleavage was obtained. After correcting for dilution, the extinction coefficients of the monomers were used to calculate the original oligomer concentration and hence extinction coefficient. The value measured is within 10% of that predicted for an oligomer with adenine replacing purine. For other sequences, the extinction coefficient was estimated by replacing purine riboside, inosine, or 2-aminopurine riboside by adenosine. In units of 10^4 M^{-1} cm^{-1}, the extinction coefficients at 280 nm are as follows: rAGCGCG, 2.83; rAGCGCGA, 3.04; rAGCGCGP, 3.04; rCGCAGGCG, 4.16; rCGCAIGCG, 4.00; rCGCPGGCG, 4.15; rGAGCGCGA, 3.82; rGCCGGAG, 3.95; rGCAAGCG, 3.36; rGCAGGCG, 3.73; rGCAIGCG, 3.50; rGCGAGCG, 3.61; rGCGPGCG, 3.37; rGCIAGCG, 3.36; rGCIPGCG, 3.60; rGCPGGCG, 3.70; rGCPPGCG, 3.30; rGC2AGCG, 3.36; rGGCGAGCC, 4.29; rGGCGPGCC, 4.25; rGPGCGCGP, 3.80; rPGCGCG, 2.80; rPGCGCGP, 3.02. Absorbance vs temperature melting curves were measured at 280 nm with a heating rate of 1.0 °C min^{-1} on a Gilford 250 spectrophotometer as described previously.[17,18] Oligomer concentration was varied over a 50- to 200-fold range.

Data Analysis. All oligomers used in this study are self-complementary. Absorbance vs temperature profiles were fit to a two-state model with sloping baselines by using a nonlinear least-squares program.[17,18] Thermodynamic parameters for duplex formation were obtained by two methods: (1) enthalpy and entropy changes from fits of individual melting curves were averaged, and (2) plots of reciprocal melting temperature (T_M^{-1}) vs the logarithm of the strand concentration (log C_T) were fit to eq 1.[49]

$$T_M^{-1} = (2.3R/\Delta H^\circ) \log C_T + \Delta S^\circ/\Delta H^\circ \quad (1)$$

Error Analysis. The error limits in Tables I and II for ΔG°_{37}, ΔH°, and ΔS° derived from fitted parameters are standard deviations. The sample covariance of ΔH° and ΔS°, $\sigma_{\Delta H^\circ \Delta S^\circ}$, can be calculated from the standard deviations in ΔG°_{37}, ΔH°, and ΔS° with the equation[50]

$$(\sigma_{\Delta G^\circ_{37}})^2 = (\sigma_{\Delta H^\circ})^2 + T^2(\sigma_{\Delta S^\circ})^2 - 2T(\sigma_{\Delta H^\circ \Delta S^\circ})^2 \quad (2)$$

where T is the temperature (Kelvin). The sample covariance, $\sigma_{\Delta H^\circ \Delta S^\circ}$, can also be calculated from the equation[50]

$$(\sigma_{\Delta H^\circ \Delta S^\circ})^2 = 1/(N-1)\sum_i[(\Delta H_i - \overline{\Delta H})(\Delta S_i - \overline{\Delta S})] \quad (3)$$

The covariances derived by these methods indicate the correlation coefficient between ΔH° and ΔS° is greater than 0.99; therefore, ΔG°_{37} is a more accurate parameter than either ΔH° or ΔS° individually.[18]

The error limits in Tables I and II for ΔH° and ΔS° derived from T_M^{-1} vs log C_T data reflect the standard deviation in the slopes and intercepts[51] with all data points weighted equally. Error in ΔH° is proportional to the standard deviation in the slope. Error in ΔS° is slightly larger than the error in ΔH° because ΔS° depends on the slope, intercept, and the covariance of the slope and intercept.[51,52] The error in ΔG°_{37} was calculated from

$$(\sigma_{\Delta G^\circ_{37}})^2 = \sigma_b^2(2.3RT/m)^2 + \sigma_m^2(-2.3R/m^2 + 2.3RTb/m^2)^2 - \sigma_{bm}^2(2.3RT/m)(-2.3R/m^2 + 2.3RTb/m^2) \quad (4)$$

where b, m, σ_b^2, σ_m^2, and σ_{bm}^2 are the y-intercept, slope, variance of intercept, variance of slope, and covariance, respectively, for eq 1. Errors in thermodynamic parameters of hydrogen bond formation were obtained from error propagation.[50] For example,

$$\sigma_{\Delta G^\circ_{37}}(\text{H-bond}) = 0.5[(\sigma_{\Delta G^\circ_{37}}(\text{GC}\underline{\text{G}}\text{AGCG}))^2 + (\sigma_{\Delta G^\circ_{37}}(\text{GC}\underline{\text{G}}\text{NGCG}))^2]^{1/2} \quad (5)$$

CD Spectroscopy. CD spectra were measured with a Jasco J-40 spectropolarimeter. The buffer was the same as for the UV melting studies. The measured CD was converted to $\Delta\epsilon$ as described by Cantor and Schimmel.[53]

(48) Borer, P. N. *Handbook of Biochemistry and Molecular Biology: Nucleic Acids*; 3rd ed.; Fasman, G. D., Ed.; CRC Press: Cleveland, OH, 1975; Vol. 1, p 597.

(49) Borer, P. N.; Dengler, B.; Tinoco, I., Jr.; Uhlenbeck, O. C. *J. Mol. Biol.* **1974**, *86*, 843–853.

(50) Bevington, P. R. *Data Reduction and Error Analysis for the Physical Sciences*; McGraw-Hill: New York, 1969.

(51) Meyer, S. L. *Data Analysis for Scientists and Engineers*; Wiley: New York, 1975; Chapter 14.

(52) Snedecor, G. W.; Cochran, W. G. *Statistical Methods*; The Iowa State University Press: Ames, IA, 1971; p 190.

(53) Cantor, C. R.; Schimmel, P. R. *Biophysical Chemistry Part II: Techniques for the Study of Biological Structure and Function*; W. H. Freeman: San Francisco, CA, 1980; Chapter 8.

Acknowledgment. We thank Philip C. Bevilacqua for suggesting the purine substitution and for stimulating discussions and Adam E. Peritz for synthesizing blocked adenosine for oligonucleotide synthesis. This work was supported by National Institutes of Health Grant GM22939. J.S.L. is an E. H. Hooker Fellow.

Registry No. 1, 133324-30-8; **2** (isomer 1), 133324-31-9; **2** (isomer 2), 133324-59-1; **3** (isomer 1), 133324-32-0; **3** (isomer 2), 133324-60-4; **4** (isomer 1), 133324-33-1; **4** (isomer 2), 133324-61-5; **5**, 70337-80-3; **6**, 133324-34-2; **7**, 133324-35-3; **8**, 133324-36-4; **9**, 133324-37-5; **10**, 133348-46-6; **11** (isomer 1), 133324-38-6; **11** (isomer 2), 133324-62-6; **12** (isomer 1), 133324-39-7; **12** (isomer 2), 133324-63-7; **13** (isomer 1), 133324-40-0; **13** (isomer 2), 133324-64-8; **14** (isomer 1), 133324-41-1; **14** (isomer 2), 133324-65-9; **15** (isomer 1), 133348-47-7; **15** (isomer 2), 133324-66-0; **16** (isomer 1), 133324-42-2; **16** (isomer 2), 133324-67-1; A, 73-24-5; G, 73-40-5; P, 120-73-0; I, 68-94-0; PTSA, 6192-52-5; TEAHF, 29585-72-6; DMTr-Cl, 40615-36-9; DMAP, 1122-58-3; TPS-Cl, 6553-96-4; DHP, 110-87-2; rGCGAGCG, 124154-71-8; rGCGPGCG, 133324-43-3; rGCIAGCG, 133324-44-4; rGCIPGCG, 133324-45-5; rGCPPGCG, 133324-46-6; rGCAAGCG, 129173-86-0; rGC2AGCG, 133348-48-8; rGCAGGCG, 129173-87-1; rGCPGGCG, 133324-47-7; rGCAIGCG, 133324-48-8; rGGCGAGCC, 129173-88-2; rGGCGPGCC, 133324-49-9; rCGCAAGCG, 121186-88-7; rCGCAGGCG, 129173-89-3; rCGCPGGCG, 133324-50-2; rCGCAIGCG, 133324-51-3; rGCGCGp, 101696-92-8; rGGCGCCP, 101696-96-2; rCGCGCGp, 99508-76-6; rAGCGCG, 133324-52-4; rPGCGCG, 133324-53-5; rAGCGCGA, 133324-54-6; rAGCGCGP, 133348-49-9; rPGCGCGP, 133324-55-7; rGAGCGCGA, 133324-56-8; rGPGCGCGP, 133324-57-9; rGCCGGAP, 101696-83-7; rGCCGGAG, 133324-58-0; rGCGC, 73942-16-2; rCCGG, 55048-62-9; 1,3-dichloro-1,1,3,3-tetraisopropyldisiloxane, 69304-37-6; isobutyric acid anhydride, 97-72-3; diisopropylethylamine, 7087-68-5; diisopropylammonium tetrazolide, 93183-36-9; bis(diisopropylamino)(β-cyanoethoxy)phosphine, 102691-36-1; 9-(2′-*o*-tetrahydropyranyl-5′-*o*-(dimethoxytrityl)-β-D-ribofuranosyl)hypoxanthine, 126647-53-8; hydrazine, 301-01-2; nebularine, 550-33-4; guanosine, 118-00-3.

Supplementary Material Available: One figure showing plots of T_M^{-1} vs log C_T for rAGCGCG, rAGCGCGA, rGGCGPGCC, rPGCGCG, rPGCGCGP, rAGCGCGP, and rGCCGGAG and one figure with circular dichroism spectra for rGCAAGCG, rGCPPGCG, rGC2AGCG, rGCCGGAG, rAGCGCGA, rAGCGCGP, and rPGCGCGP (2 pages). Ordering information is given on any current masthead page.

Communications to the Editor

Observation of an Unprecedented Equilibrium between Alkyl–Carbonyl, η^2-Acyl, and Agostic Acyl Isomeric Structures†

Ernesto Carmona,* Leopoldo Contreras, Manuel L. Poveda, and Luis J. Sánchez

Departamento de Química Inorgánica
Instituto de Ciencia de Materiales
Universidad de Sevilla-CSIC
Apdo 553, 41071 Sevilla, Spain

Received December 10, 1990

Bidentate acyl coordination is very commonly encountered among the early transition metals,[1] including the 6d metals.[2-5] Recent studies carried out in this[5] and other laboratories[6,7] have demonstrated the existence of fast equilibria between η^2-acyl complexes and their isomeric alkyl–carbonyl formulations (structures B and A, respectively). On the other hand, an earlier contribution[3b] from our group has provided an unprecedented acetyl, $Mo(\overline{C(O)CH_3})(S_2CNMe_2)(CO)(PMe_3)_2$ (**1**), in which there is a strong agostic interaction[8] between the metal center and one of the acetyl β-C–H bonds (structure C).

Scheme I

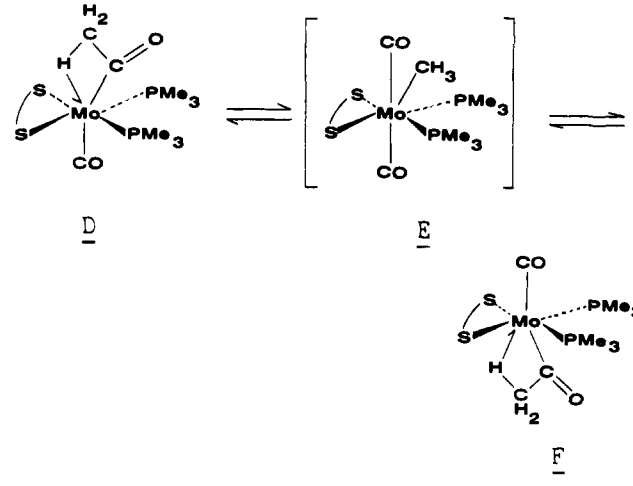

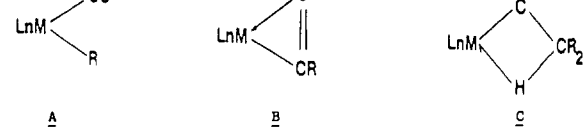

† Dedicated to Professor R. Usón on the occasion of his retirement.

(1) (a) Fachinetti, G.; Fochi, G.; Floriani, C. *J. Chem. Soc., Dalton Trans.* **1977**, 1946. (b) Marsella, J. A.; Moloy, K. G.; Caulton, K. G. *J. Organomet. Chem.* **1980**, *201*, 389. (c) Manriquez, J. M.; McAlister, D. R.; Sanner, R. D.; Bercaw, J. E. *J. Am. Chem. Soc.* **1976**, *98*, 6733; **1978**, *100*, 2716. (d) Wolczanski, P. T.; Bercaw, J. E. *Acc. Chem. Res.* **1980**, *13*, 121. (e) Erker, G. *Acc. Chem. Res.* **1984**, *17*, 103 and references therein. (f) Calderazzo, F. *Angew. Chem., Int. Ed. Engl.* **1977**, *89*, 299. (g) For a recent review of M–η^2-acyl complexes, see: Durfee, L. D.; Rothwell, I. P. *Chem. Rev.* **1988**, *88*, 1059.

(2) (a) Rusik, C. A.; Collins, M. A.; Gamble, A. S.; Tonker, T. L.; Templeton, J. L. *J. Am. Chem. Soc.* **1989**, *111*, 2550. (b) Curtis, M. D.; Shiu, K. B.; Butler, W. M. *J. Am. Chem. Soc.* **1986**, *108*, 1550.

(3) (a) Carmona, E.; Wilkinson, G.; Rogers, R. D.; Hunter, W. E.; Zaworotko, M. J.; Atwood, J. L. *J. Chem. Soc., Dalton Trans.* **1980**, 229. (b) Carmona, E.; Sánchez, L.; Marin, J. M.; Poveda, M. L.; Atwood, J. L.; Riester, R. D.; Rogers, R. D. *J. Am. Chem. Soc.* **1984**, *106*, 3214. (c) Carmona, E.; Contreras, L.; Sánchez, L.; Gutiérrez-Puebla, E.; Monge, A. *Inorg. Chem.* **1990**, *29*, 700. (d) Carmona, E.; Muñoz, M. A.; Rogers, R. D. *Inorg. Chem.* **1988**, *27*, 1598. (e) Carmona, E.; Marin, J. M.; Poveda, M. L.; Sánchez, L.; Rogers, R. D.; Atwood, J. L. *J. Chem. Soc., Dalton Trans.* **1983**, 1003.

(4) (a) Bonnesen, P. V.; Yau, P. K. L.; Hersh, H. W. *Organometallics* **1987**, *6*, 1587. (b) Sunkel, K.; Schloter, K.; Beck, W.; Ackermann, K.; Schubert, U. *J. Organomet. Chem.* **1983**, *241*, 333. (c) Kreissl, F. R.; Sieber, W. J.; Keller, H.; Riede, J.; Wolfgruber, M. *J. Organomet. Chem.* **1987**, *320*, 83. (d) Ali, H. G. *J. Organomet. Chem.* **1977**, *127*, 349.

(5) (a) Carmona, E.; Sánchez, L. J. *Polyhedron* **1988**, *7*, 163. (b) Carmona, E.; Contreras, L.; Poveda, M. L.; Sánchez, L. J.; Atwood, J. L.; Rogers, R. *Organometallics* **1991**, *10*, 61. (c) Carmona, E.; Contreras, L.; Gutiérrez-Puebla, E.; Monge, A.; Sánchez, L. J. *Organometallics* **1991**, *10*, 71.

(6) Roper, W. R.; Taylor, G. E.; Waters, J. M.; Wright, L. J. *J. Organomet. Chem.* **1979**, *182*, C46.

(7) Jablonsky, C.; Bellachioma, G.; Cardaci, G.; Reichenbach, G. *J. Am. Chem. Soc.* **1990**, *112*, 1632.

(8) Brookhart, M.; Green, M. L. H.; Wong, L. L. *Prog. Inorg. Chem.* **1988**, *36*, 1.

0002-7863/91/1513-4322$02.50/0